Journal of Research in Environmental Science and Toxicology Vol. 1(4) pp. 66-90, May 2012
Available online http://www.interesjournals.org/JREST

Full Length Research Paper

The effect of functional parameters on microbial characteristics in crude oil degradation

Ukpaka C. P.

Department of Chemical/Petrochemical Engineering
Rivers State University of Science and Technology,
Nkpolu, P.M.B. 5080, Port Harcourt., Nigeria.
E-mail: chukwuemeka24@yahoo.com

Accepted 02 March, 2012

In this research work contains experimental and theoretical data obtained from the results. The crude oil sample obtained in Niger Delta Area of Nigeria was subjected in isolation and identification of possible microorganism, present on it. The microorganisms were cultured and subject to different temperature effect of 20^{o}C, 40^{o}C, 60^{o}C, 80^{o}C and 100^{o}C. The variation in temperature influences the crude composition and characteristic such as viscosity, density and surface tension. As the functional parameters changes the microbial activity changes as well in the bioreactor. The temperature of the bioreactor influence the viscosity, density, surface tension and microbial growth rate, most of the microorganisms in the bioreactor attain it optimum growth rate within the temperature of 40^{o}C to 60^{o}C. Comparing the experimental and theoretical data obtained shows a good match indicating that either the experimental or theoretical developed model can be used in monitoring and predicting the effect of temperature on biodegradation of crude oil. The various microorganisms used for this investigation include: *pseudomonas alcaligenes, pseudomonas mendocina, pseudomonas stutzeri, pseudomonas veronica and pseudomonas putida* and only *pseudomonas alcaligenes* withstand temperature above 80^{o}C, indicating its effectiveness on enhancing bioremediation at high operating temperature. The mathematical model developed was used to establish the LinearWeaver Burk plot which was useful in determining the specific growth rate, maximum specific growth rate and the equilibrium constant.

Keywords: Effect, Functional Parameters, Microbial, Characteristics, Crude Oil, Degradation.

INTRODUCTION

Oil exploration and its associated activities have caused significant damage and threat to the environment, which has resulted in health and ecological problems.

It is therefore pertinent, to develop effective technological methods to address the harms done to the environment. There exist different innovative technological methods of handling pollution problems, but the bioremediation method has received considerable attention because of its environmental friendly nature, moreso, it is cost effective. Bioremediation is any process that uses microorganisms, fungi, green plants or their enzymes to return the natural environment altered by contaminants to its original condition (Daugulis and McCracken, 2003; Leahy and Cohwell, 1990; Atlas, 1981; Adebusoye, Ilori, Amund, Teniola and Olatope, 2007; Das and Mukherjee, 2007; Ukpaka, 2007 and Brooijmans, Pastink,and Siezen, 2009).

A better understanding of the nature, characteristics and adaptive features of petroleum hydrocarbon-degrading microbial community offers an improved strategy for oil-spill remediation. This project (Research work) is intended to ascertain the effect of temperature on the characteristic of hydrocarbon-degrading microorganisms (microbes). At certain temperature regime some microbes grow and reproduce optimally, this is called the optimal operating temperature (favourable temperature condition), of the microbes(Atlas and Bartha, 1992; Foght and Westlake, 1987; Prince, 1993; Bae *et al*, 2002; Chailian *et al*,2004 and Barth and Bossert, 1984).

The characteristics of upper and lower temperature limits which is a function of the metabolism of the microbes, this has their survival boundary, therefore any temperature condition below or above the microbe's optimal temperature range will cause a denaturing of the microbes which is detrimental to a successful bioremediation exercise. Micro- organisms are divided into groups based on where their optimal growth temperature falls(Bhat, Tsuda, Horiike, Nozaki, Vaidyanathan and Nakazawa, 1994; Ukpaka, 2005 and Holliger, Gaspard and Glod, 1997). The grouping is only an approximation that sets temperature boundary conditions necessary to predict microbial characteristics as a function of temperature. The various groups of the operational temperature is given as: Extreme psychophilic (Psychotrophs) temperature below 5^oC; Mesophilic temperature of 25^oC to 45^oC; Thermopilic temperatures of 45^oC to 75^oC; Extreme or super-thermophilics; temperature above 70^oC; A successful oil spill bioremediation process is dependent on one's ability to identify and maintain conditions that favours oil spill (hydrocarbon contaminant) biodegradation rate in contaminated environment (Ukpaka and Nnadi, 2008).

The use of micro-organism with the appropriate metabolic capacities is the first step to achieving a successful bioremediation. Microbial degradation process (Bioremediation) aids the elimination of spilled oil from the environment after critical removal of a large volume of the oil (contaminant) by different physical and chemical methods. The use of microbes in crude oil degradation is possible because of the presence of enzyme systems in micro organisms which degrade and utilize different hydrocarbons as a source of energy (Ukpaka, 2011).

Generally, bioremediation is the use of micro-organisms to detoxify or remove pollutants owing to their diverse metabolic capacities. It has been established, that there are limiting factors that affect the biodegradation of petroleum hydrocarbons, some of which are: composition and inherent biodegradability of the hydrocarbon pollutant; temperature; pH condition; nutrients concentration; inhibitor; oxygen concentration; solubility; moisture content; these functional parameters mention above at times act as an activator and inhibitor to the bioreactors contaminants etc.

Some of these limiting factors directly affect the chemistry of the containments as well as affecting the physiology and diversity of the microbial flora (Ukpaka, 2010).

It is also necessary to check how these other factors affect biodegradation in a temperature regime. Thus, this research work is carried out to ascertain the effect of temperature on the biodegradation of crude oil, as a result of alteration in microbial characteristics. The primary aim of this study is to determine the effects of functional parameters on the characteristics of hydrocarbon-degrading microbial community. The aims of this research work (Project) can be summarize as follows: determination of functional parameters effects on microbial characteristic in crude oil degradation; determination of microbial growth behavior (growth profile) as a function of the change in functional parameters; establishment of optimum operating temperature condition, at which the microbial degrading ability is optimal; determination of the effect of functional parameters change with respect to other limiting factors on microbial growth characteristics; development of a mathematical model that can predict this functional parameters (Ukpaka, 2009).

The significance of this research work is in its critical study of the effect of functional parameters temperature on the microbial species involved in crude oil degradation. At some functional parameters conditions, some micro-organism which takes part in biodegradation is very effective. Thus, the need to know the different microbial species present in an environment in order to afford the bioremediation process the optimal and effective operating temperature condition. The relative resistance of heavy hydrocarbons to degradation at low temperature conditions calls for in depth understanding on how to simulate or manipulate temperature to favour biodegradation process in cold marine environment like the Niger - Delta Region. An effective and active temperature conditions reduces the inhibitory tendencies of crude oil to biodegradation.

There are different factors that affect effective bioremediation process, but the objective of this study (research work) focuses on the effect of functional parameters on the hydrocarbon-degrading micro-organisms. It is the objective of this research work to establish a relationship between temperature and microbial growth behavior in order to achieve a successful bioremediation process. It is also desired by this research work to establish the effect of temperature in relation with other factors that affect bioremediation of polluted environment. This research work contributes to knowledge in way of drawing up reliable relationship between temperature and microbial growth profile (i.e. effect on their cellular and metabolic processes). This knowledge of the relationship, contribute to the success of any bioremediation exercise to be carried out in any contaminated area.

The scope of this work is based on the effect of functional parameters on microbial characteristics in the biodegradation of crude oil (petroleum hydrocarbons). This involves the analysis of the biodegradation rate of the hydrocarbons in relation to the microbial growth profile (growth rate/ decay rate) as a function of the change in temperature conditions (This temperature effect is also measured against other environment factors, such as pH, oxygen content), nutrient concentration and the composition and biodegradability of the petroleum hydrocarbon pollutants.

MATERIALS AND METHODS

Mathematical Model Development

The degree rise in temperature per-unit time, affects the microbial characteristics as well as their growth rate which also affect the rate of biodegradation. The equation of the temperature below predicts the effect of change in temperature in reaction rate per unit time.

$$\frac{dT}{dt} = KT \tag{1}$$

Integrating both sides of the equation gives

$$\int dT = \int kT(dt)$$

$$\int_{T_{\min}}^{T_{opt}} = kT\int_0^t dt$$

$$\text{In } [\mathrm{T}]_{T_{\min}}^{T_{opt}} = kT[t]_0^t$$

$$\text{In } [\mathrm{T_{opt}} - T_{\min}] = kT[t-0]$$

$$\text{In}\frac{\mathrm{T_{opt}}}{\mathrm{T_{min}}} = kTt = T_{\min}e^{-kT(t)} \tag{2}$$

where, T_{opt} = optimal temperature for biodegradation; T_{min} = minimum temperature for biodegradation; T = test temperature for biodegradation; t = time of biodegradation; k = first-order rate constant which is dependent on the biodegradability of the hydrocarbon specie.

$$T_{opt} = T_{\min}e^{-kT(t)} \tag{3}$$

From the Michealis-menten equation, the microbial growth rate is given by

$$U_m = U_{max(T)} = \frac{S}{K_m + S} \tag{4}$$

where, U_T = specific growth rate at temperature T; $U_{max(T)}$ = maximum specific growth rate at the temperature T; S = substrate concentration; K_m = Michaelis constant

Using the temperature equation as an inhibitory factor the microbial growth rate in the Michaelis-menten equation i.e. combining equation (3) and (4)

$$U_T = U_{\max(T)}\frac{S}{K_m + S} \bullet T_{\min}e^{-kT(t)} \tag{5}$$

The parameters are as defined previously. Equation (5) is the relationship between the change in temperature and its effect on the microbial growth kinetics (microbial characteristic). From the non-linear regression model which is used to determine the relationship between the concentration hydrocarbon species and the number of colonies of microbial population (Biomass concentration), that can grow on it. The model equation is given as;

$$S = \frac{A}{e^{(k-x)}} \tag{6}$$

where, S = concentration of hydrocarbon (mg/L); A = a theoretical value of maximum concentration of hydrocarbon, the microbial species can use as source of carbon; X = biomass concentration (number of colonies). The Levenberg-marquardt model a non-linear least squares method is used to calculate the A and k parameters.

The combination of equation (5) and (6) can be used to predict the growth rate of microbial species with the hydrocarbon (substrate0 concentration i.e. making microbial growth rate a function of biomass concentration.

Recalling $U_T = U_{\max(T)}\frac{S}{K_m + S} \bullet T_{\min}e^{-kT(t)}$ and $S = \frac{A}{e^{(k-x)}}$

On combination of equation (5) and (6) gives

$$U_T = U_{\max(T)}\frac{\frac{A}{e^{(k-x)}}}{K_m + \frac{A}{e^{(k-x)}}} \bullet T_{\min}e^{-kT(t)} \tag{7}$$

Moreso, from the Gompertz model equation which is a non-linear relationship between temperatures effect and the time of biodegradation is given as;

$$q = Ae^{-\left[e^{(-kk_m t)}\right]} \tag{8}$$

where, q = percentage of hydrocarbon biodegraded at a specific temperature; t = time of biodegradation; A = a theoretical value of maximum value of hydrocarbon that can be biodegraded; K_m = model parameter. The Quasi-Newton method is used to calculate the model parameters (A and K). If the rate of biodegradation is dependent on the temperature and the specific growth rate of the microbial population then equations (7) and (8) be used to model a temperature-microbial growth-biodegradation model as follows:

$$q = Ae^{-\left[e^{(-k_m t)}\right]} \bullet U_{\max(T)}\frac{A/e^{(k-x)}}{k_m + \frac{A}{e^{(k-x)}}} \bullet T_{\min}e^{-kT(t)} \tag{9}$$

Table 1. Result of analysis microbial of functional parameters (temperature, density, API gravity, viscosity and surface tension as well as microbial growth).

Parameters	Concentration of the parameters					
Temperature ^oC	15.6	20	40	60	80	100
Density (g/ml)	0.899	0.898	0.876	0.850	0.820	0.785
API gravity (^{o}API)	25.9	26.1	30.0	35.0	41.1	48.8
Viscosity (CP)	2.52	2.48	2.09	1.86	1.62	1.37
Surface tension (dyness/cm)	27.50	27.48	25.64	24.55	23.10	22.00
P. alcaligenes x 10^3 cfu/m (P.A.)	1.8	2.6	5.4	6.1	2.2	0.3
P. mendocina x 10^3 cfu/ml (P.M)	1.1	2.0	4.3	4.9	0.2	0
P. Stutzeri x 10^3 cfu/ml (P.S)	2.4	3.2	6.8	4.1	0	0
P. Veronii (P.V) x 10^3cfu/ml	3.3	4.0	5.3	1.2	0	0
P. Putida (P.P) x 10^3 cfu/ml	2.0	2.7	6.6	3.9	0.5	0

Table 2. Result of analysis on the effect of temperature on microbial population.

Parameters	Temperature ^oC					
Micro-organisms x 10^3 cfu/ml	15.6^{o}C	20^{o}C	40^{o}C	60^{o}C	80^{o}C	100^{o}C
(P.A) *pseudomonas alcaligenes*	1.8	2.6	5.4	6.1	2.2	0.3
(P.M) *pseudomonas mendocina*	1.1	2.0	4.3	4.9	0.0	0
(P.S) *pseudomonas Stutzeri*	2.4	3.2	6.8	4.1	0	0
(P.V) *pseudomonas Veronii*	3.3	4.0	5.3	1.2	0	0
(P.P) *pseudomonas putida*	2.0	2.7	6.6	3.9	0.5	0

Table 3. Result of analysis on the some of functional parameters.

Parameters	Concentration of the parameter					
Temperature ^oC	15.6^{o}C	20^{o}C	40^{o}C	60^{o}C	80^{o}C	100^{o}C
Density (g/ml)	0.899	0.898	0.876	0.850	0.820	0.785
API gravity (^{o}API)	25.9	26.1	30.0	35.0	41.1	48.8
Viscosity (CP)	2.52	2.48	2.09	1.86	1.62	1.37
Surface tension (dynes/Cu)	27.50	27.48	25.64	24.55	23.10	22.00

Table 4. Result of analysis of specific growth rate of *pseudomonas alcaligenes* (P.A.) with density as function of substrate.

Tem. ^oC	Density (S) g/ml	Specific rate of P.A. (h^{-1}) μ x 10^3	$\frac{1}{S}(ml/g)^{-1}$	$\frac{1}{\mu}$ (h)
15.6	0.899	0.075	1.1124	13.33
20	0.898	0.108	1.1136	9.26
40	0.876	0.225	1.1416	4.44
60	0.850	0.254	1.1765	3.94
80	0.820	0.0917	1.2195	10.91
100	0.785	0.0125	1.2739	80.00

where q is a function of U_T and T.
Equation (9) can be reduced to

$$q = Ae^{-\left[e^{(-k_m t)}\right]} \bullet U_{\max(T)} \frac{1}{k_m} T_{\min} e^{-kT(t)} \quad (10)$$

Experimental Procedures

Apparatus used

The following apparatus were used in carrying out the

Table 5. Analysis of the specific rate of growth of P.A. due to API gravity as function of substrate.

Temperature °C	API gravity °API (S)	Specific rate of growth of P.A. (h^{-1}) $\mu \times 10^3$	$\frac{1}{S}$	$\frac{1}{\mu}$ (h)
15.6	25.9	0.075	0.0386	13.33
20	26.1	0.108	0.0383	9.26
40	30.0	0.225	0.0333	4.44
60	35.0	0.254	0.0286	3.94
80	41.1	0.0917	0.0243	10.91
100	48.8	0.0125	0.0205	80.00

Table 6. Result of analysis of the specific growth rate of P.A upon the influence of surface tension as function of substrate.

Tem. °C	Surface tension dynes/cm [S]	Rate of growth of P.A. (h^{-1}) $\mu \times 10^3$	$\frac{1}{S}$	$\frac{1}{\mu}$
15.6	27.50	0.075	0.0364	13.33
20	27.48	0.108	0.0364	9.26
40	25.64	0.225	0.0390	4.44
60	24.55	0.254	0.0407	3.94
80	23.10	0.0917	0.0433	10.91
100	22.00	0.0125	0.0455	80.00

Table 7. Result of analysis of the specific growth rate of pseudomonas mendocina (P.M) upon the influence of density as function of substrate.

Tem. °C	Density g/ml (S)	Specific growth of P.M. (μ) $h^{-1} \times 10^3$	$\frac{1}{S}$	$\frac{1}{\mu}$ (h)
15.6	0.899	0.046	1.1124	21.74
20	0.898	0.083	1.1136	12.01
40	0.876	0.179	1.1416	5.59
60	0.850	0.204	1.1765	4.90
80	0.820	0.008	1.2195	125
100	0.785	0	1.2739	0

Table 9. Result of analysis of the specific growth rate (h^{-1}) of P.M. due to API gravity as function of substrate.

Tem. °C	API gravity °API [S]	Specific growth of P.M. (h^{-1}) $\mu \times 10^3$	$\frac{1}{S}$	$\frac{1}{\mu}$
15.6	25.9	0.046	0.0386	21.74
20	26.1	0.083	0.0383	12.01
40	30.0	0.179	0.0333	5.59
60	35.0	0.204	0.0286	4.90
80	41.1	0.008	0.02343	125
100	48.8	0	0.0205	0

Table 10. Result of analysis of the specific growth of *pseudomonas mendocina* (P.M.) upon the influence of surface tension.

Tem. °C	Surface tension dynes/cm [S]	Rate of growth of P.M. (h^{-1}) μ x 10^3	$\frac{1}{S}$	$\frac{1}{\mu}$
15.6	27.50	0.046	0.0364	21.74
20	27.48	0.084	0.0364	12.01
40	25.64	0.179	0.0390	5.59
60	24.55	0.204	0.0407	4.90
80	23.10	0.008	0.0433	125
100	22.00	0	0.0455	0

Table 11. Result of analysis of the specific growth rate of *pseudomonas stutzeri* (P.S) due to density as a function of substrate.

Tem. °C	Density g/ml (S)	Specific rate of growth of P.S. (h^{-1}) μ x 10^3	$\frac{1}{S}$	$\frac{1}{\mu}$
15.6	0.899	0.10	1.112	10.0
20	0.898	0.13	1.114	7.7
40	0.876	0.26	1.142	3.9
60	0.850	0.17	1.177	5.9
80	0.820	0	1.220	0
100	0.785	0	1.274	0

Table 12. Result of analysis of the specific growth of *pseudomonas statzeri* (P.S.) due to viscosity as a function of substrate.

Tem. °C	Surface tension dynes/cm [S]	Rate of growth of P.V. (h^{-1}) μ x 10^3	$\frac{1}{S}$	$\frac{1}{\mu}$
15.6	2.52	0.10	0.400	10.0
20	2.48	0.13	0.403	7.7
40	2.09	0.26	0.479	3.9
60	1.86	0.17	0.585	5.9
80	1.62	0	0.617	0
100	1.37	0	0.730	0

Table 13. Result of analysis of the specific growth rate (h^{-1}) of *pseudomonas stutzeri* (P.S) upon the influence of API gravity as a function of substrate.

Tem. °C	API gravity °API [S]	Specific growth of P.S (h^{-1}) μ x 10^3	$\frac{1}{S}$	$\frac{1}{\mu}$
15.6	25.9	0.10	0.0386	10.0
20	26.1	0.13	0.0383	7.7
40	30.0	0.26	0.0333	3.9
60	35.0	0.17	0.0286	5.9
80	41.1	0	0.0243	0
100	48.8	0	0.0205	0

Table 14. Result of analysis of specific growth of *pseudomonas stutzeri* (P.S) (h^{-1}) upon the influence of surface tension as a function of substrate.

Tem. °C	Surface tension dynes/ cm [S]	Specific growth of P.S (h^{-1}) μ x 10^3	$\frac{1}{S}$	$\frac{1}{\mu}$
15.6	27.50	0.10	0.0364	10.0
20	27.48	0.13	0.0364	7.7
40	25.64	0.26	0.0390	3.9
60	24.55	0.17	0.0407	5.9
80	23.10	0	0.0433	0
100	22.00	0	0.0455	0

Table 15. Result of analysis of the specific growth of *pseudomonas veronii* (P.V) due to influence of density as a function of substrate.

Tem. °C	Density g/ml (S)	Specific rate of growth of P.V (h^{-1}) μ x 10^3	$\frac{1}{S}$	$\frac{1}{\mu}$
15.6	0.899	0.138	1.112	7.25
20	0.898	0.167	1.114	5.99
40	0.876	0.221	1.142	4.53
60	0.850	0.05	1.177	20
80	0.820	0	1.220	0
100	0.785	0	1.274	0

Table 16. Result of analysis of the specific growth of *pseudomonas veronii* (P.V) due to viscosity.

Tem. °C	Viscosity (CP) (S)	Specific rate of growth of P.V. (h^{-1}) μ x 10^3	$\frac{1}{S}$	$\frac{1}{\mu}$
15.6	2.52	0.138	0.400	7.25
20	2.48	0.167	0.403	5.99
40	2.09	0.221	0.479	4.53
60	1.86	0.05	0.538	20.00
80	1.62	0	0.617	0
100	1.37	0	0.730	0

Table 17. Result of analysis of the specific rate of growth of *pseudomonas veronii* (P.V) due to API gravity as a function of substrate.

Tem. O°C	API gravity °API [S]	Specific rate of growth of P.V. (h^{-1}) μ x 10^3	$\frac{1}{S}$	$\frac{1}{\mu}$
15.6	25.9	0.138	0.0386	7.25
20	26.1	0.167	0.0383	5.99
40	30.0	0.221	0.0333	4.53
60	35.0	0.05	0.0286	20
80	41.1	0	0.0243	0
100	48.8	0	0.0205	0

research work such as: petri dishes, measuring cylinder, pipette, glass spreader, griffin 105 incubator, laboratory

Table 18. Result of analysis of the Specific rate of growth of *pseudomonas veronii* (P.V) upon influence of surface tension as a function of substrate.

Tem. °C	Surface tension dynes (Cm) (S)	Specific rate of growth of P.V. (h^{-1}) μ x 10^3	$\frac{1}{S}$	$\frac{1}{\mu}$
15.6	27.50	0.138	0.0364	7.25
20	27.48	0.167	0.0364	5.99
40	25.64	0.221	0.0390	4.53
60	24.55	0.05	0.407	20
80	23.10	0	0.0433	0
100	22.00	0	0.0455	0

Table 19. Result of analysis of the specific growth rate of *pseudomonas pitida* (P.P) due to the Influence of density as a function of substrate.

Tem. °C	density g/ml (S)	Specific rate of growth of P.P. (h^{-1}) μ x 10^3	$\frac{1}{S}$	$\frac{1}{\mu}$
15.6	0.899	0.083	1.112	12.05
20	0.898	0.113	1.114	8.065
40	0.976	0.275	1.142	3.64
60	0.850	0.163	1.177	6.14
80	0.820	0.021	1.220	47.62
100	0.785	0	1.274	0

Table 20. Result of analysis of the specific growth rate of *pseudomonas putida* (P.P.) due to viscosity as a function of substrate.

Tem. °C	Viscosity (CP) (S)	Specific rate of growth of P.P. (h^{-1}) μ x 10^3	$\frac{1}{S}$	$\frac{1}{\mu}$
15.6	2.52	0.083	0.400	12.05
20	2.48	0.113	0.403	8.85
40	2.09	0.275	0.479	3.64
60	1.86	0.163	0.538	6.14
80	1.62	0.021	0.617	37.62
100	1.37	0	0.730	0

oven

Reagents and Media

The following reagents and media were used in carrying out the research work such as: crude oil [Mogho oil field in Gokana], normal saline, and nutrient agar (broth medium)

Procedures

1ml of crude oil was diluted in 9ml of normal saline (0.85g of NaCl diluted in 1litre of distill water). This is the first dilution which is 10^{-1}, the second and third dilution was done to enable effective and proper counting of the bacteria species and population. A serial dilution was done in the following order 1st dilution was 1ml of crude oil dilution in 9ml of normal saline (10^{-2}) and the third dilution was 1ml of second dilution in 9ml of normal saline (10^{-3}), 10^{-1} for 1st dilution, 10^{-2} for 2nd dilution and 10^{-3} for 3rd dilution are called dilution factor, 0.1ml of the third dilution (innoculant) was inoculated in a growth media (broth medium), the innoculant was spreaded with a glass spreader in the Petri dish. The following are the micro-organisms identified: *pseudomonas alcaligenes (p.alcaligenes), pseudomonas mendocina (p.mendocina), pseudomonas stutzer (p.stutzeri), pseudomonas veronii (p.veronii), pseudomonas putida (p.pudida).* The initial

Table 21. Result of analysis of the specific rate of growth of *pseudomonas putida* (P.P.) due to API gravity as a function of substrate.

Tem. °C	AIP gravity °API	Specific rate of growth of P.P. (h^{-1}) μ x 10^3	$\frac{1}{S}$	$\frac{1}{\mu}$
15.6	25.9	0.083	0.0386	12.05
20	26.1	0.113	0.0383	8.85
40	30.0	0.275	0.0333	3.64
60	35.0	0.163	0.0286	6.14
80	41.1	0.021	0.0243	47.62
100	48.8	0	0.0205	0

Table 22. Result of analysis of the specific rate of growth of *pseudomonas putida* (P.P.) upon the influence of surface tension as a function of substrate.

Tem. O°C	Surface tension dynes (cm) [S]	Specific rate of growth of P.P. (h^{-1}) μ x 10^3	$\frac{1}{S}$	$\frac{1}{\mu}$
15.6	27.50	0.083	0.0364	12.05
20	27.48	0.113	0.0364	8.85
40	25.64	0.275	0.0390	3.64
60	24.55	0.163	0.0401	6.14
80	23.10	0.021	0.0433	47.62
100	22.00	0	0.0455	0

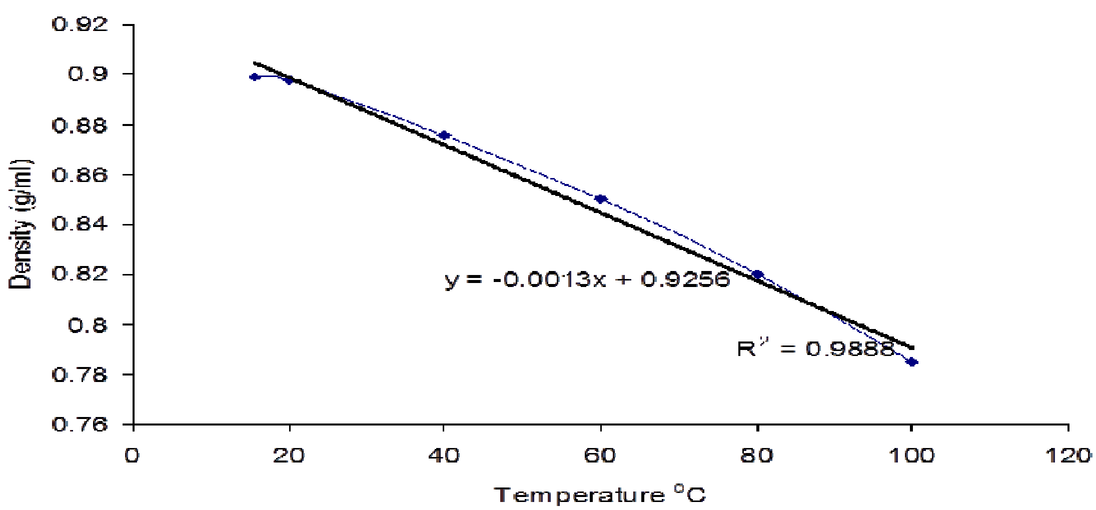

Figure 1. Graph of Density against temperature

population of the various species was counted and recorded the ehavi forming unit (cfu/ml) 1-S given by the relation

$$\text{Cfu/ml} = \frac{\textit{Total number of colony}}{} \times \textit{Reciprocal of dilution factor} \times \textit{Volume plated}$$

For this particular experiment the volume plated is 0.1 and the dilution factor is 10^{-3}

The initial population of the different species was counted before incubating at the following temperatures: 20°C, 40°C, 60°C, 80°C and 100°C and the growth at each temperature was recorded to demonstrate the effect of temperature on microbial characteristics in terms of their growth ehavior. The incubation was done for 24 hours.

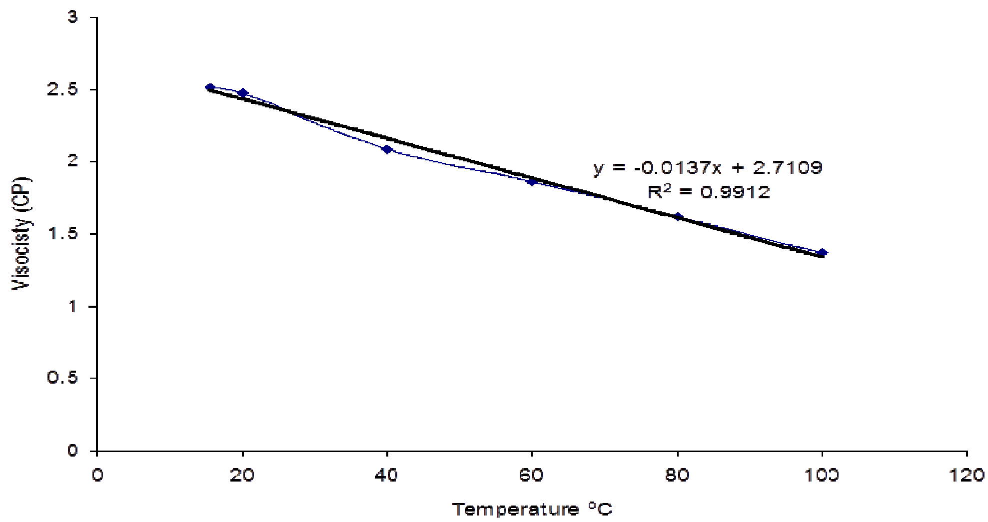

Figure 2. Graph of viscosity against temperature

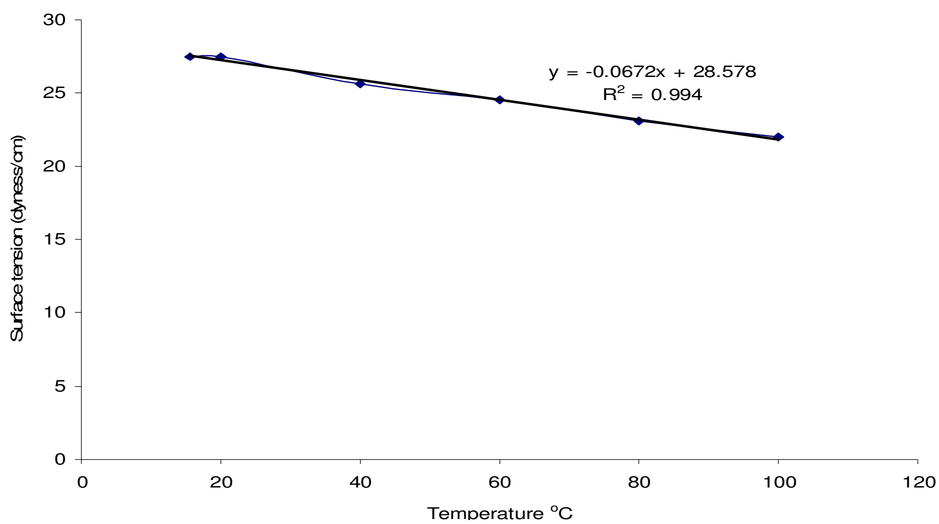

Figure 3. Graph of surface tension against temperature

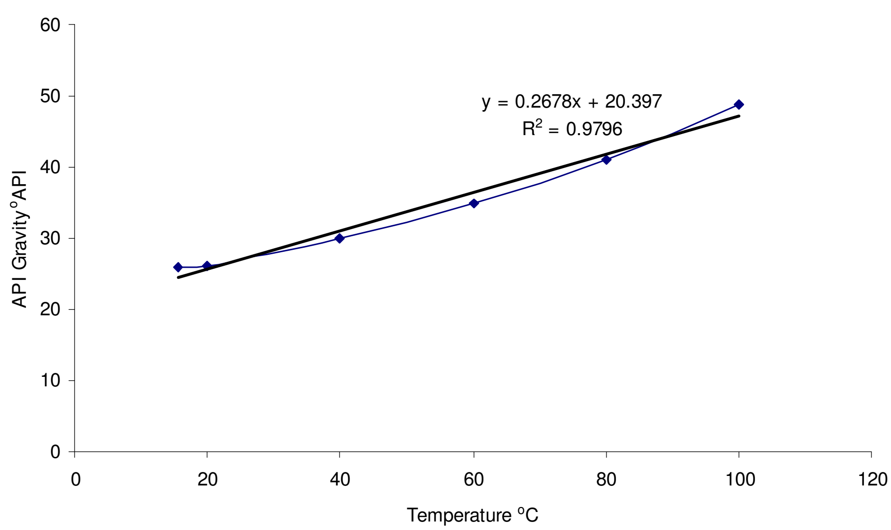

Figure 4. Graph of API gravity against temperature

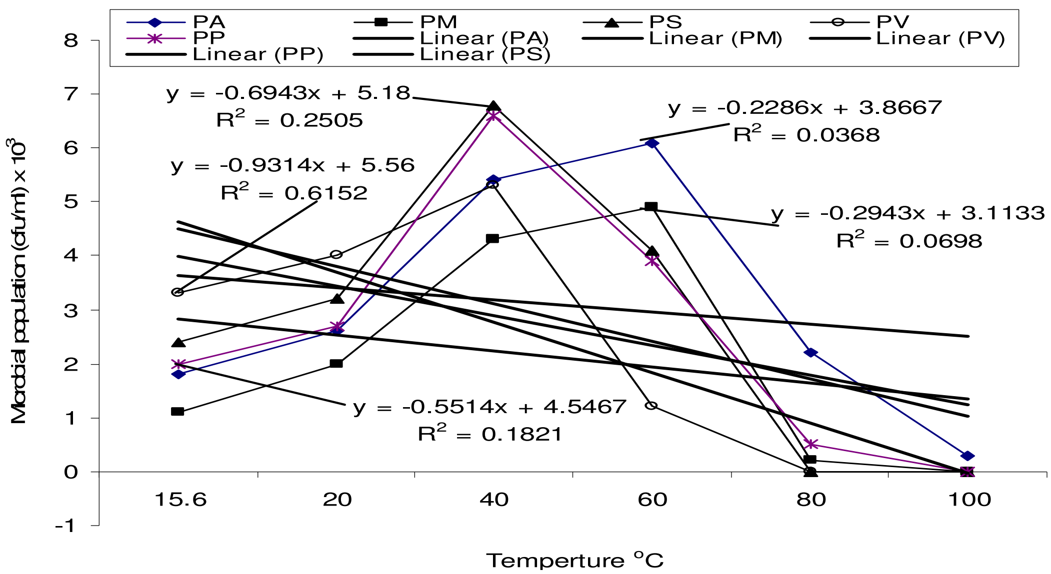

Figure 5. Graph of microbial growth against temperature

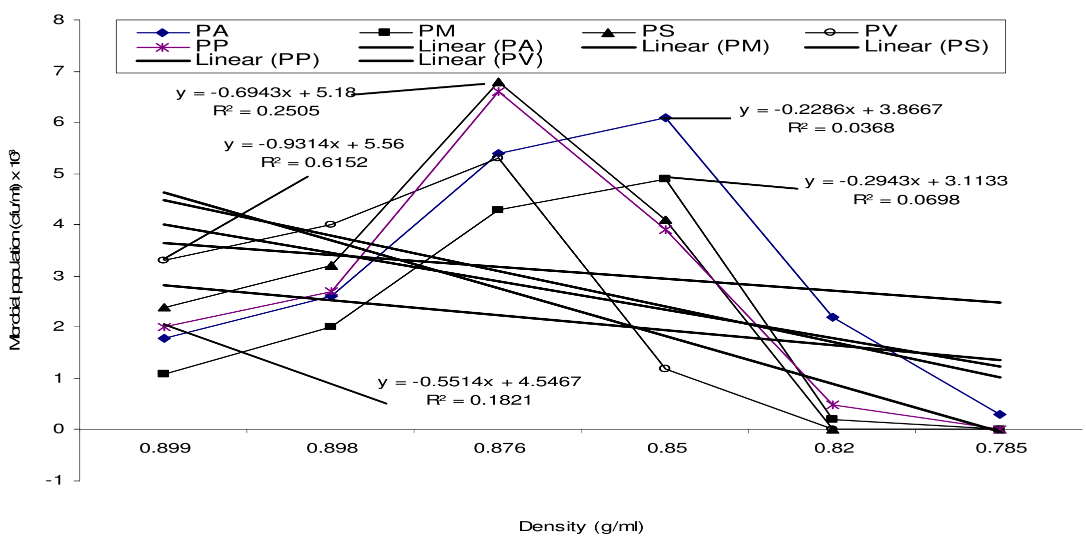

Figure 6. Graph of microbial growth against density (g/ml).

RESULTS AND DISCUSSION

Results obtained from the investigation are presented in Tables and Figures as shown:

The result presented in Figure 1, illustrate the relationship between temperature and density, as the temperature increases the density decreases. The equation of best fit and the square root of the curve is given as y = -0.0013x + 0.9256 and R^2 = 0.9888.

Figure 2 shows the relationship between temperature and viscosity. As the temperature increases the viscosity decreases. This indicates an inverse relationship existing between the two parameters. Therefore, y = -0.0137x + 2.7109 and R^2 = 0.9912 are the equation of best fit and square root of the curve respectively.

Figure 3 demonstrates the relationship between temperature and surface tension. An increase in temperature causes decrease in surface tension. The equation of the best fit is given as y = -0.0672x + 28.578 and R^2 = 0.994.

The relationship between temperature and API gravity is establish by Figure 4. It is observed that as the temperature increases, the equation of best fit is given as y = 0.2678x + 20.397 and R^2 = 0.9796.

Result in Figure 5 illustrates the relationship between temperature and growth of the different pseudomonas species. All the pseudomonas species experienced growth at 40°C, this indicates that their optimal growth region lies within 40°C - 60°C. The equation of best fit and square root of the curves for each curve is given

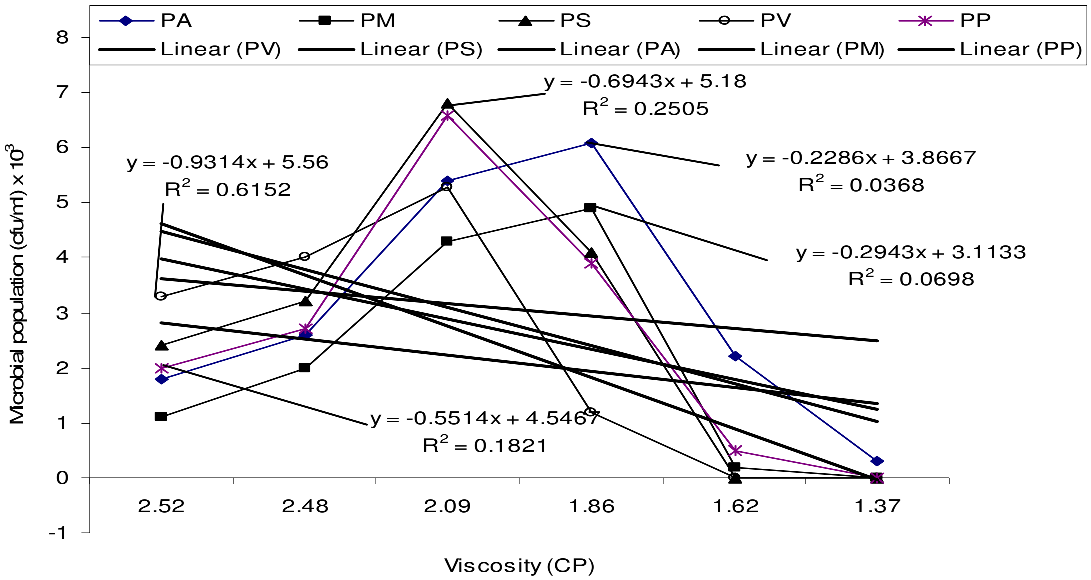

Figure 7. Graph of microbial growth against viscosity.

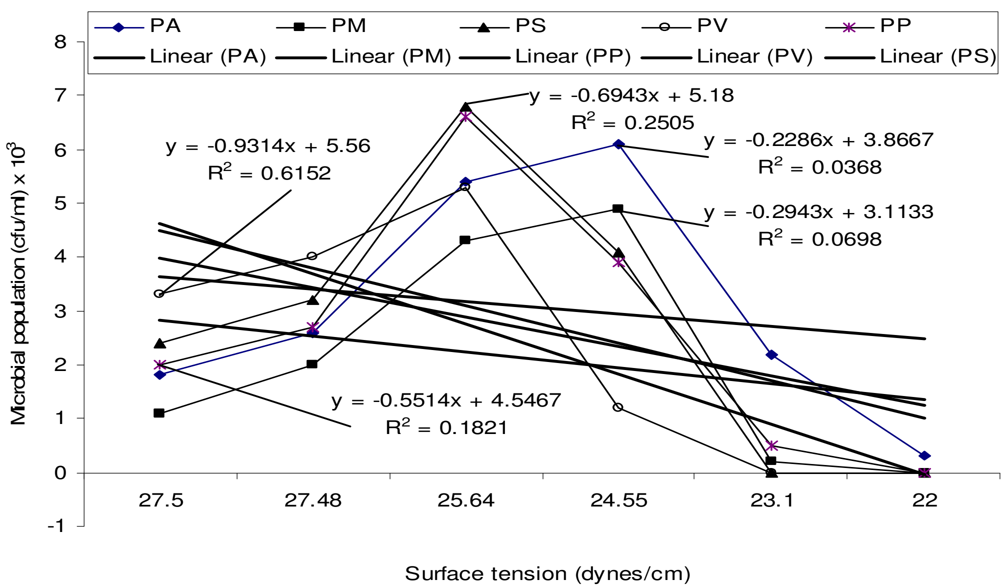

Figure 8. Graph of microbial growth against Surface tension (dynes/cm).

below:

PA: y = -0.02286x + 3.8667, and R^2 = 0.0368; PM: y = -0.2943x + 3.113, and R^2 = 0.0698; PV: y = -0.6943x + 5.18, and R^2 = 0.6152; PP: y = -0.9314x + 5.56, and R^2 = 0.1821 PS: y = -0.5514x + 4.5467,

and R^2 = 0.2505.

The result presented in Figure 6, demonstrates density – microbial growth relationship. Initially, as the density decreases there was considerable increase in the growth of the pseudomonas species. But at a point, the decrease in density saw a corresponding decrease in growth.

PA: y = -0.02286x + 3.8667, and R^2 = 0.0368; PM: y = -0.2943x + 3.113, and R^2 = 0.0698; PV: y = -0.6943x + 5.18, and R^2 = 0.6152; PP: y = -0.9314x + 5.56, and R^2 = 0.1821; PS: y = -0.5514x + 4.5467, and R^2 = 0.2505; are the equations of best fit and square roots for each pseudomonas specie.

The result presented in Figure 7 is graphical illustration of the relationship between viscosity and microbial growth. All the pseudomonas species experience increase in growth with decreasing viscosity. And experience sudden decline in growth with decreasing viscosity, this shows that the relationship is a quasi one.

The equation of best fit and square roots of the curves

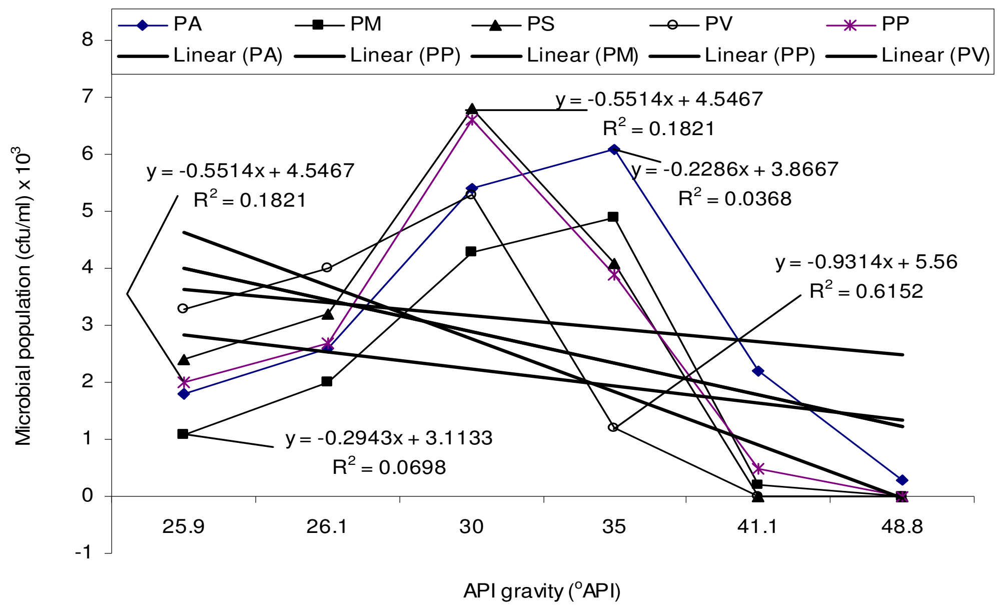

Figure 9. Graph of microbial growth against API gravity.

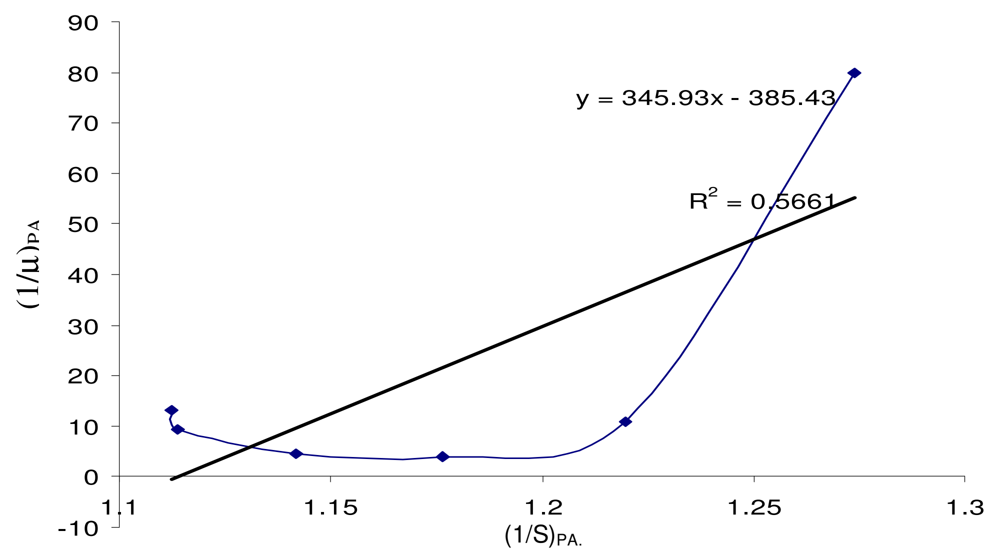

Figure 10. Graph of Line Weaver Burk plot of 1/µ versus 1/S for P.A. of density dependent.

For all the pseudomonas species are given as:

PA: $y = -0.02286x + 3.8667$, and $R^2 = 0.0368$; PM: $y = -0.2943x + 3.113$, and $R^2 = 0.0698$; PV: $y = -0.6943x + 5.18$, and $R^2 = 0.6152$; PP: $y = -0.9314x + 5.56$, and $R^2 = 0.1821$; PS: $y = -0.5514x + 4.5467$, and $R^2 = 0.2505$

Figure 8 illustrate the relationship between surface tension and the growth of the microbial population. An initial decrease surface tension causes increase in the growth of the microbial population. However, a point was reached, when decrease in surface tension causes decrease in growth.

PA: $y = -0.02286x + 3.8667$, and $R^2 = 0.0368$; PM: $y = -0.2943x + 3.113$, and $R^2 = 0.0698$; PV: $y = -0.6943x + 5.18$, and $R^2 = 0.6152$; PP: $y = -0.9314x + 5.56$, and $R^2 = 0.1821$; PS: $y = -0.5514x + 4.5467$, and $R^2 = 0.2505$; are the equations of best fit and square roots of the curves for various pseudomonas specie.

Figure 9, demonstrate the relationship between microbial growth and API gravity. It is observed that as the API gravity increases, the microbial population also increases, until a point is reached, when in further increase. In API gravity result in decrease in microbial growth, the equations of best fit and square root of the curves are shown below:

PA: $y = -0.02286x + 3.8667$, and $R^2 = 0.0368$; PM:

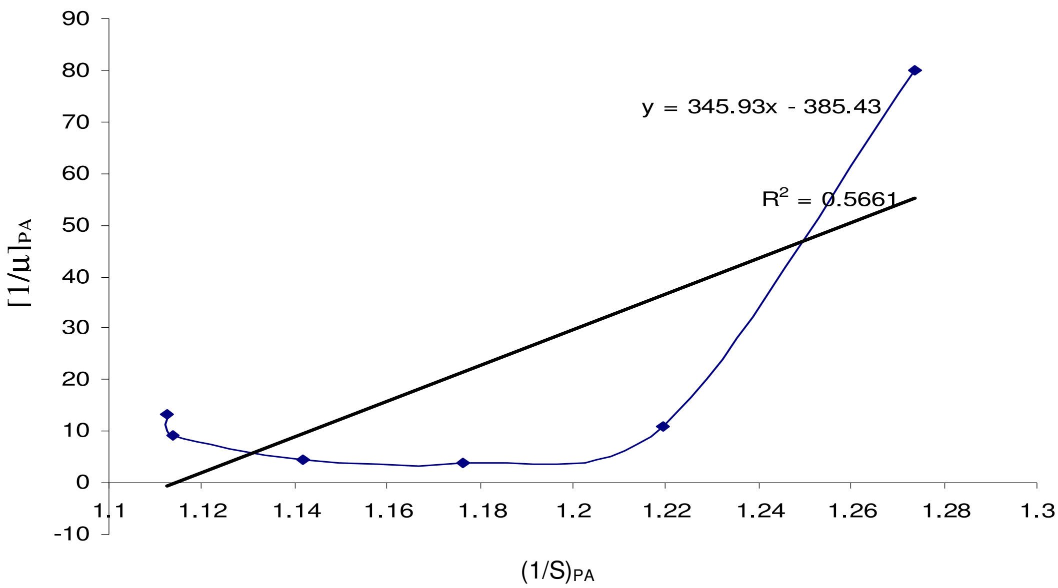

Figure 11. Graph of Line Weaver Burk plot of 1/μ versus 1/S for P.A. of viscosity dependent.

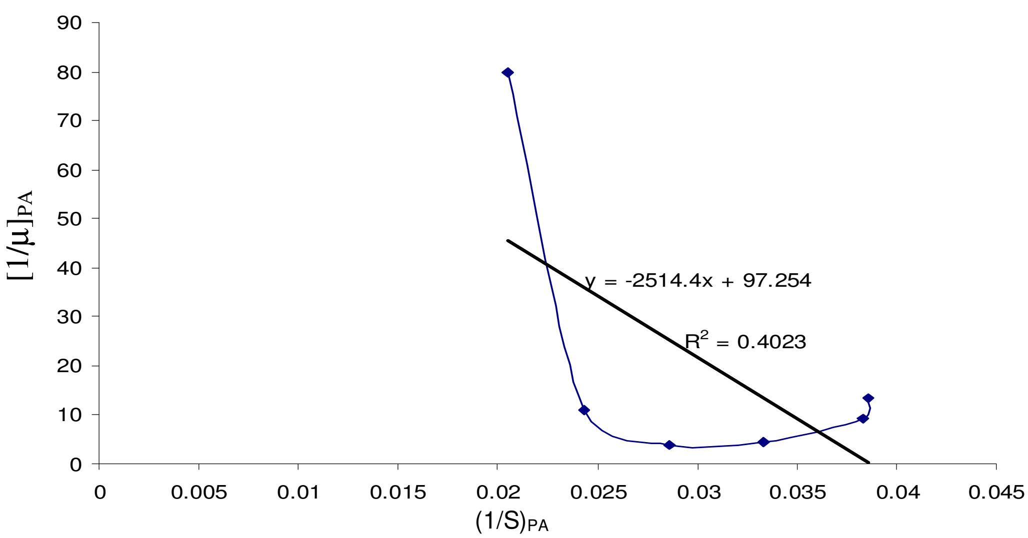

Figure 12. Graph of Line Weaver Burk plot of 1/μ versus 1/S for P.A. of API gravity dependent.

y = -0.2943x + 3.113, and R^2 = 0.0698; PV: y = -0.6943x + 5.18, and R^2 = 0.6152; PP: y = -0.9314x + 5.56, and R^2 = 0.1821; PS: y = -0.5514x + 4.5467, and R^2 = 0.2505.

The result presented in Figure 10 established the relationship between $\left[\frac{1}{\mu}\right]_{PA}$ and $\left[\frac{1}{S}\right]_{PA}$ for density dependent. It is observed that a stationary point exist within 1.15 – 1.21, before increasing. The relationship between $\left[\frac{1}{\mu}\right]_{PA}$ and $\left[\frac{1}{S}\right]_{PA}$ is not perfectly linear the square of best fit is given as y = 345.93x – 385.43 with square root R^2 = 0.5561.

Figure 11 establishes the relationship between $\left[\frac{1}{\mu}\right]_{PA}$ and $\left[\frac{1}{S}\right]_{PA}$ for viscosity dependent. Initial increase in $\left[\frac{1}{S}\right]_{PA}$ resulted in stationary behaviour of $\left[\frac{1}{\mu}\right]_{PA}$ until a point was attained, when an increased observed $\left[\frac{1}{\mu}\right]_{PA}$.

Y = 345.93x – 385.48 and R^2 = 0.5661 are the equation

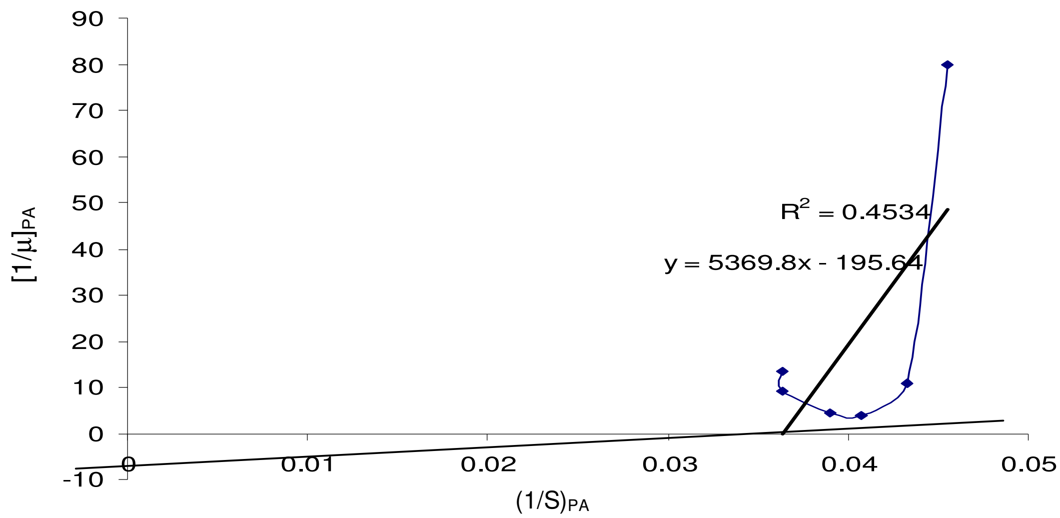

Figure 13. Graph of Line Weaver Burk plot of 1/μ versus 1/S for P.A. of surface tension dependent.

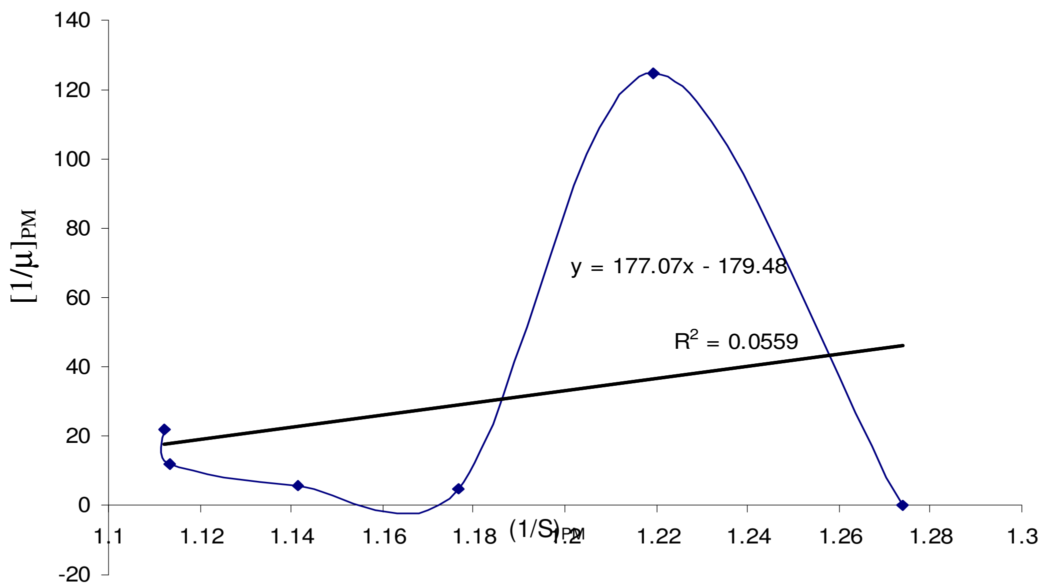

Figure 14. Graph of Line Weaver Burk plot of 1/μ versus 1/S for density dependent

best fit and square root of the curved.

The result presented in Figure 12 illustrates the relationship between $\left[\frac{1}{\mu}\right]_{PA}$ and $\left[\frac{1}{S}\right]_{PA}$ for API gravity dependent. It is observed that as $\left[\frac{1}{S}\right]_{PA}$ increases, there was an increase in $\left[\frac{1}{S}\right]_{PA}$. The equation of best fit and curves are as shown below: y=-2514.4x + 97.254. Figure 13 is the relationship between $\left[\frac{1}{\mu}\right]_{PA}$ and $\left[\frac{1}{S}\right]_{PA}$ for surface tension dependent. It is observed that as $\left[\frac{1}{S}\right]_{PA}$ is increasing there is no linear response from $\left[\frac{1}{\mu}\right]_{PA}$. However, the highest value of $\left[\frac{1}{\mu}\right]_{PA}$ is at the

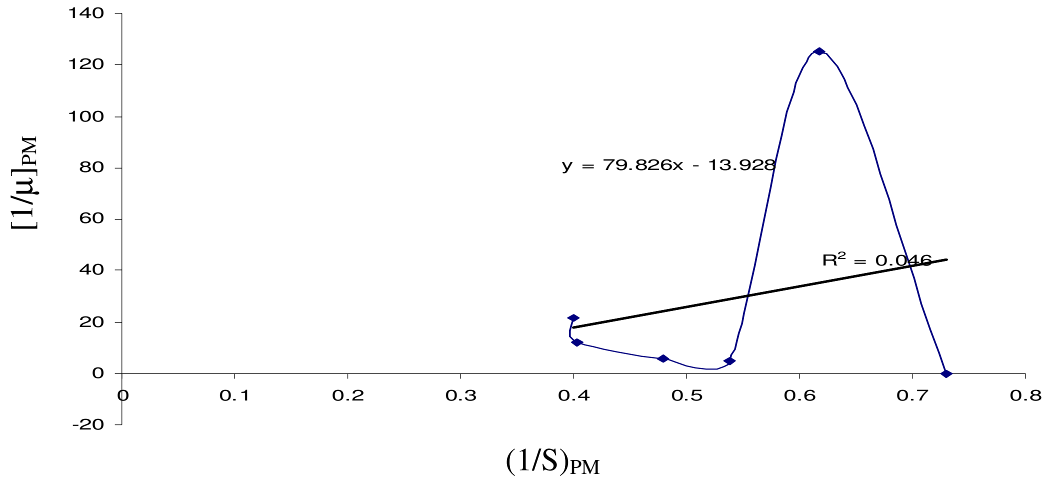

Figure 15. Graph of Line Weaver Burk plot of 1/μ versus 1/S for viscosity dependent

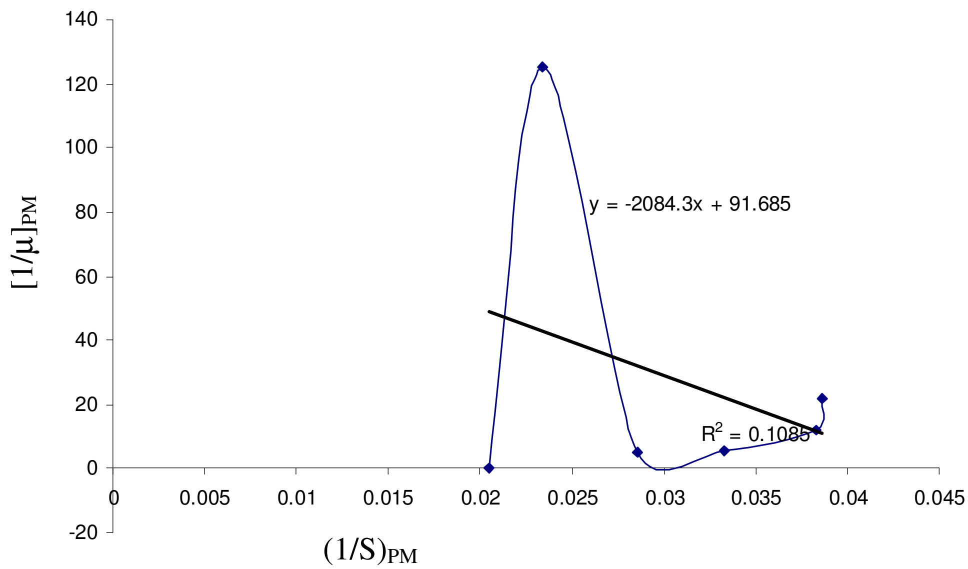

Figure 16. Graph of Line Weaver Burk plot of 1/μ versus 1/S for °API gravity dependent

highest value of $\left[\frac{1}{S}\right]_{PA}$, the equation of best fit is given as y = 5369.8x – 195.64 with square root R^2 = 0.4534.

Result presented in Figure 14 illustrate the relationship between $\left[\frac{1}{\mu}\right]_{PM}$ and $\left[\frac{1}{S}\right]_{PM}$. For density dependent, decrease in $\left[\frac{1}{\mu}\right]_{PM}$ was observed within the range of 1.12 to 1.17 and later increase to attain optimum value of $\left[\frac{1}{\mu}\right]_{PM}$ = 120 and the variation in $\left[\frac{1}{\mu}\right]_{PM}$ can be attributed to the variation in $\left[\frac{1}{S}\right]_{PM}$, the equation of best fit is y = 177.07x – 179.48 with square root of the curve equal to R^2 = 0.0559.

Figure 15 demonstrate $\left[\frac{1}{S}\right]_{PM}$ and $\left[\frac{1}{\mu}\right]_{PM}$ relationship, for viscosity dependent. Figure 15 exhibit

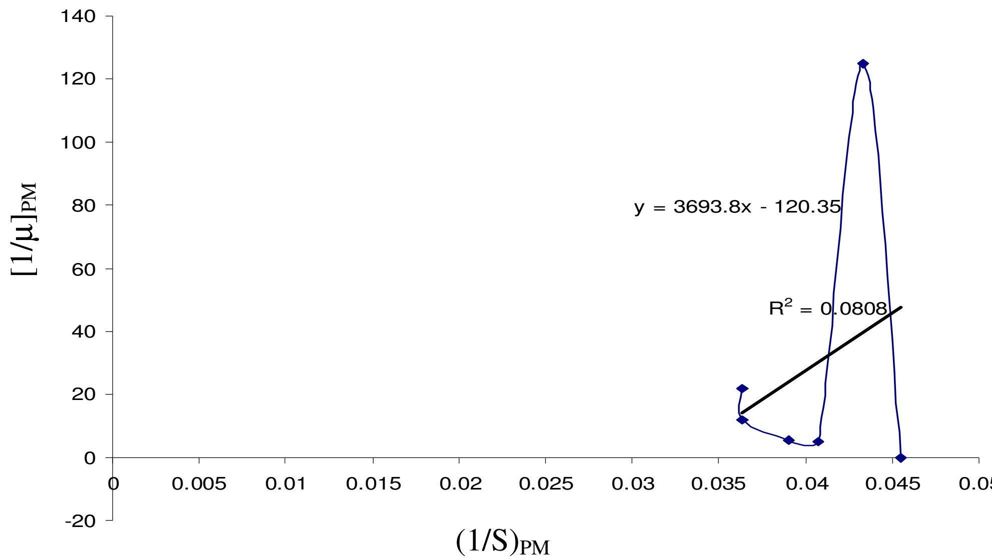

Figure 17. Graph of Line Weaver Burk plot of 1/µ versus 1/S for surface tension dependent

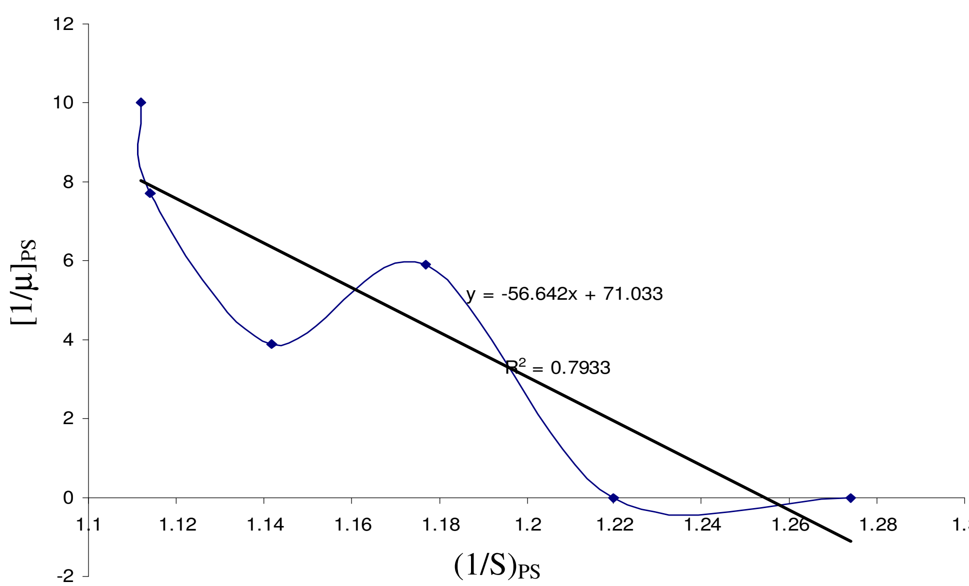

Figure 18. Graph of Line Weaver Burk plot of 1/µ versus 1/S for density dependent

similar ehavior with figure 4.14 and also has its optimum value of $\left[\frac{1}{\mu}\right]_{PM}$ at 120. Y = 79.826x - 13.928 and R^2 = 0.046, are the equation of best fit and square roots of the curve respectively.The illustration of the relationship between $\left[\frac{1}{\mu}\right]_{PM}$ and $\left[\frac{1}{S}\right]_{PM}$ for API gravity dependent is shown in Figure 16. The value of $\left[\frac{1}{\mu}\right]_{PM}$ against $\left[\frac{1}{S}\right]_{PM}$ increases to the optimum point (120) and start decreasing. The equation of best fit and square root of the curve is given below y = -2084.3x + 91.685 and R^2 =\ 0.1085.

Result presented in Figure 17 illustrate the relationship $\left[\frac{1}{\mu}\right]_{PM}$ and $\left[\frac{1}{S}\right]_{PM}$ for surface tension dependent. The

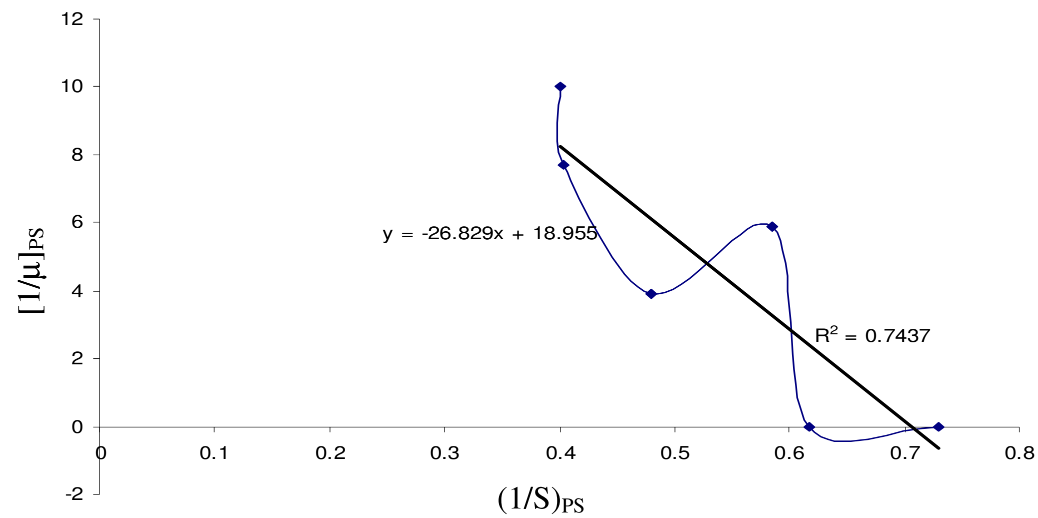

Figure 19. Graph of Line Weaver Burk plot of 1/μ versus 1/S for surface tension dependent

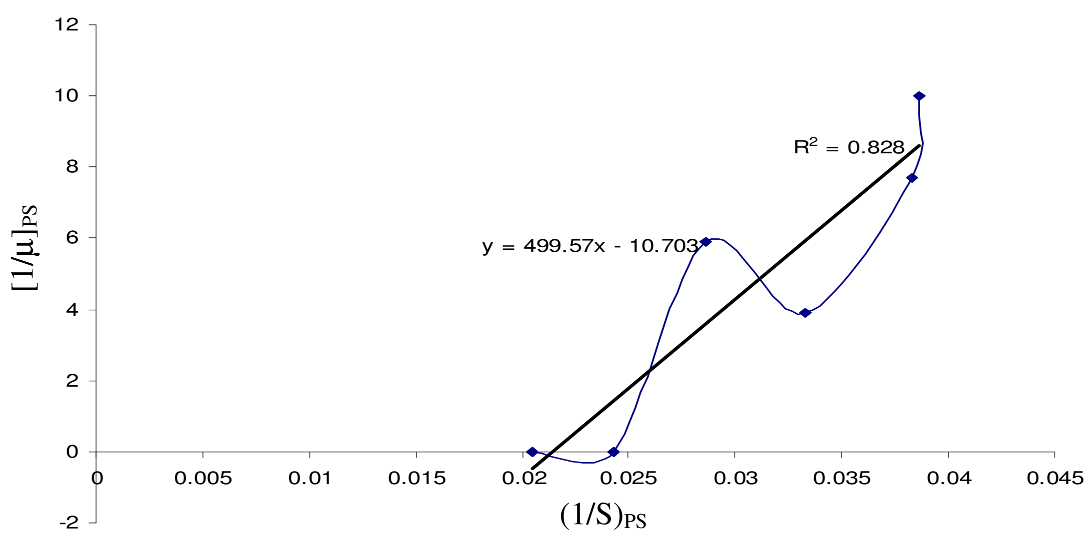

Figure 20. Graph of Line Weaver Burk plot of 1/μ versus 1/S for API gravity dependent

optimum value of $\left[\frac{1}{\mu}\right]_{PM}$ is 120 and also shown similar behaviour. Y = 3693.8x – 120.35 and R^2 = 0.0808 are the equation of best fit and square root of the curve.

Figure 18 establishes the relationship $\left[\frac{1}{\mu}\right]_{PS}$ and $\left[\frac{1}{S}\right]_{PS}$ for density dependent. The relationship takes a wave. (Crest and trough) pattern which indicates the fact that, there is no linear relationship between $\left[\frac{1}{\mu}\right]_{PS}$ and $\left[\frac{1}{S}\right]_{PS}$, y = -56.642x + 71.033 and R^2 = 0.7933, are the equation of best fit and square root of the curve.

The result of Figure 19, illustrates the relationship between $\left[\frac{1}{\mu}\right]_{PS}$ and $\left[\frac{1}{S}\right]_{PS}$. For surface tension dependent

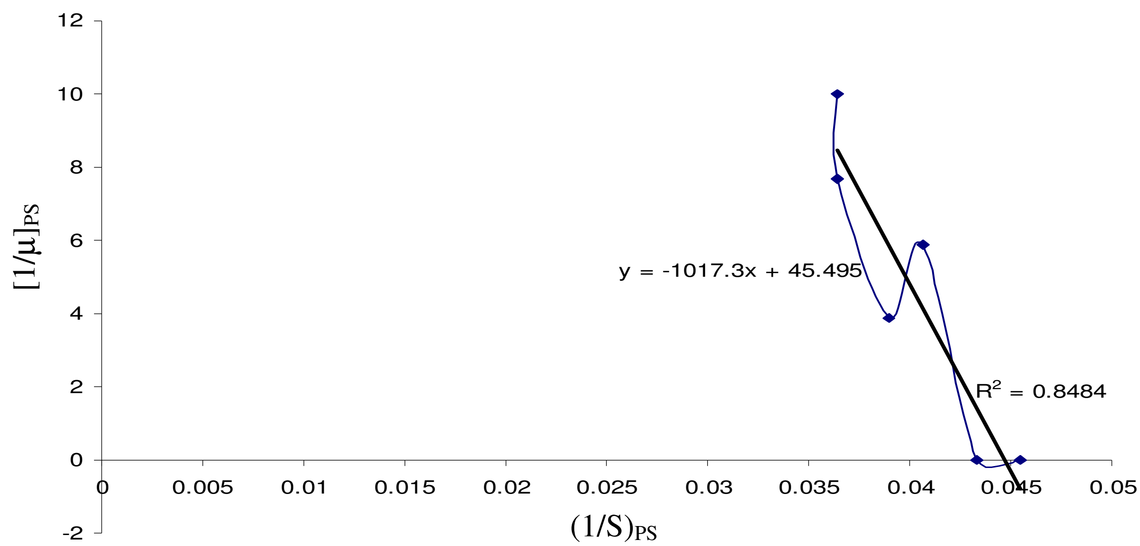

Figure 21. Graph of Line Weaver Burk plot of 1/μ versus 1/S for surface tension dependent

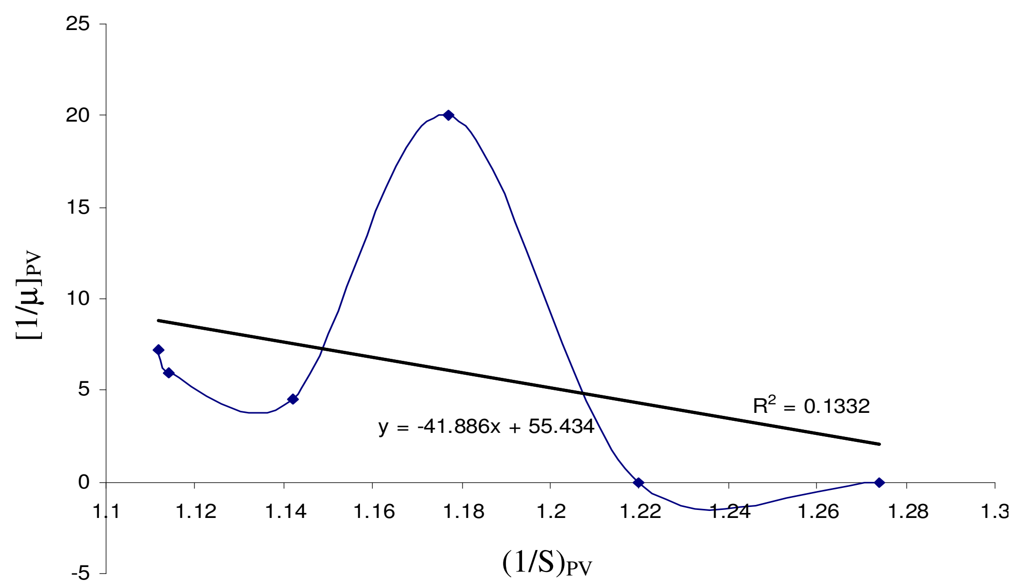

Figure 22. Graph of Line Weaver Burk plot of 1/μ versus 1/S for density dependent

The relation between $\left[\frac{1}{\mu}\right]_{PS}$ and $\left[\frac{1}{S}\right]_{PS}$ is not linear, but notably, the optimum value of $\left[\frac{1}{\mu}\right]_{PS}$ at 10 intercept with the minimum value of $\left[\frac{1}{S}\right]_{PS}$, y = -26.829x + 18.955 and R^2 = 0.7437, are the equation of best fit and square root of the curve.

The relationship between $\left[\frac{1}{\mu}\right]_{PS}$ and $\left[\frac{1}{S}\right]_{PS}$ for API gravity dependent is established by the result presented in Figure 20. From the graph, it is observed that the optimum value of $\left[\frac{1}{\mu}\right]_{PS}$ coincides with the maximum value of $\left[\frac{1}{S}\right]_{PS}$. The equation of best fit is given as y = 499.57x – 10.703 with the square root of the curve equal

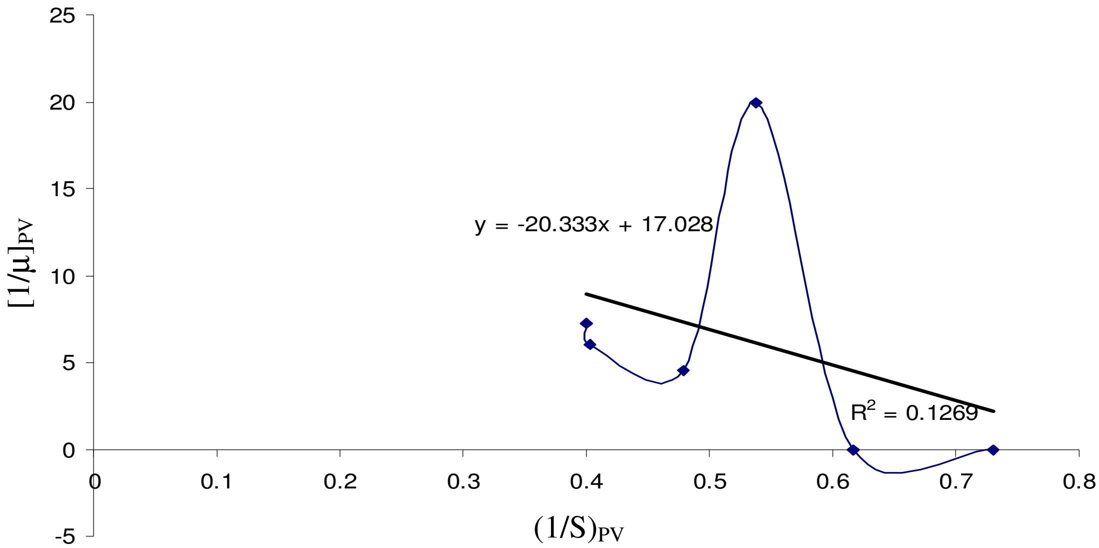

Figure 23. Graph of Line Weaver Burk plot of 1/µ versus 1/S for viscosity dependent

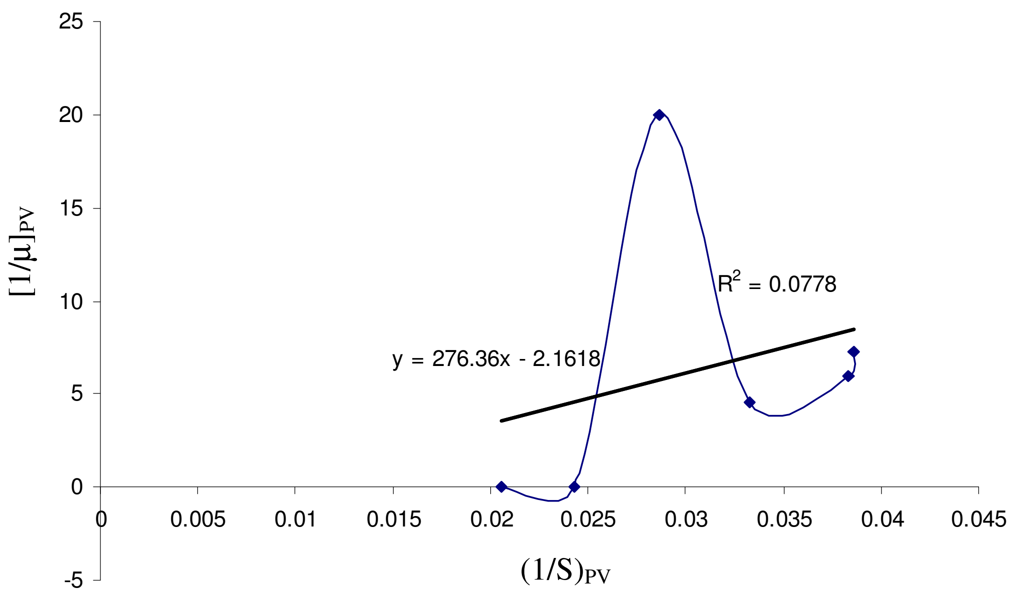

Figure 24. Graph of Line Weaver Burk plot of 1/µ versus 1/S for API gravity dependent

to R^2 = 0.828.

The result presented in Figure 21 illustrates the relationship between $\left[\frac{1}{\mu}\right]_{PS}$ and $\left[\frac{1}{S}\right]_{PS}$ for surface tension dependent. It is observed from the graph that the optimum value of $\left[\frac{1}{\mu}\right]_{PS}$ (10) is obtained at the minimum value of $\left[\frac{1}{S}\right]_{PS}$, y = -1017.3x + 45.495 and R^2 = 0.8484, are the equation of best fit and square root of the curve.

Figure 22, demonstrates the relationship between $\left[\frac{1}{\mu}\right]_{PV}$ and $\left[\frac{1}{S}\right]_{PV}$ for density dependent increase in

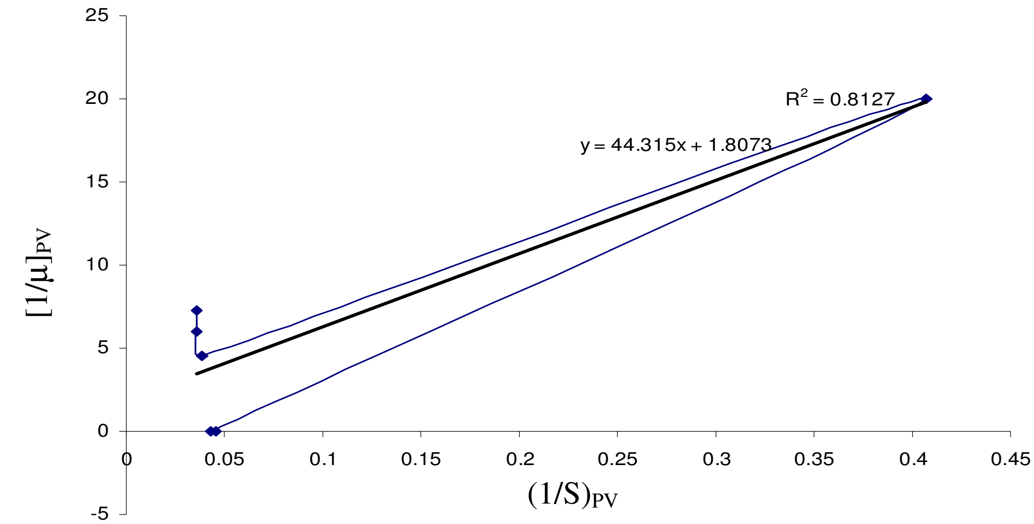

Figure 25. Graph of Line Weaver Burk plot of 1/µ versus 1/S for surface tension dependent

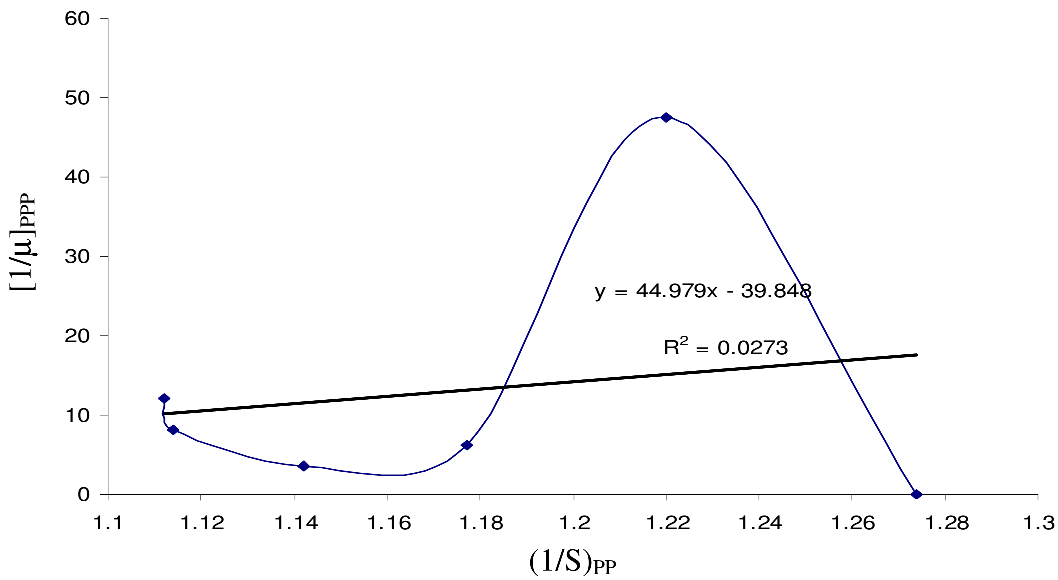

Figure 26. Graph of Line Weaver Burk plot of 1/µ versus 1/S for viscosity dependent

$\left[\frac{1}{\mu}\right]_{PV}$ was observed with 1.14 to 1.18 and later decrease from 1.18 to 1.27, the optimum value of $\left[\frac{1}{\mu}\right]_{PV}$ at 20 is obtained at 1.18. The equation of best fit is given as y = -41.886x + 55.434 with square root R^2 = 0.1332.

The result in Figure 23 demonstrates the relationship between $\left[\frac{1}{\mu}\right]_{PV}$ and $\left[\frac{1}{S}\right]_{PV}$ for viscosity dependent. An initial decrease in $\left[\frac{1}{\mu}\right]_{PV}$ was observed within 0.4-0.5, with a later increase in $\left[\frac{1}{\mu}\right]_{PV}$ at 0.55. However, further decrease was observed within 0.55 to 0.6. The optimum value of $\left[\frac{1}{\mu}\right]_{PV}$ at 20 is gotten at 0.54. y = -20.333x + 17.028 and R^2 = 0.1269 are the equation of best fit and square root of the curve.

Figure 24, illustrate the relationship between

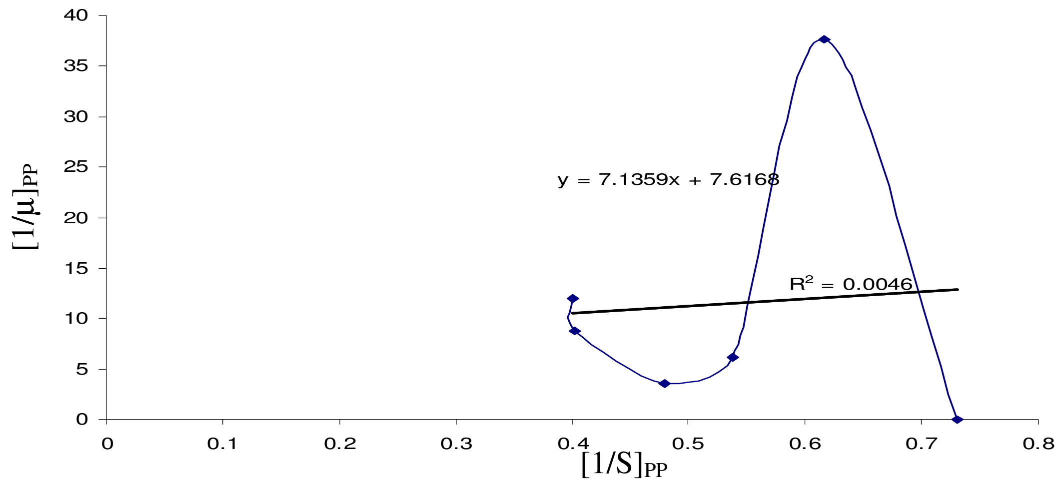

Figure 27. Graph of Line Weaver Burk plot of 1/µ versus 1/S for density dependent

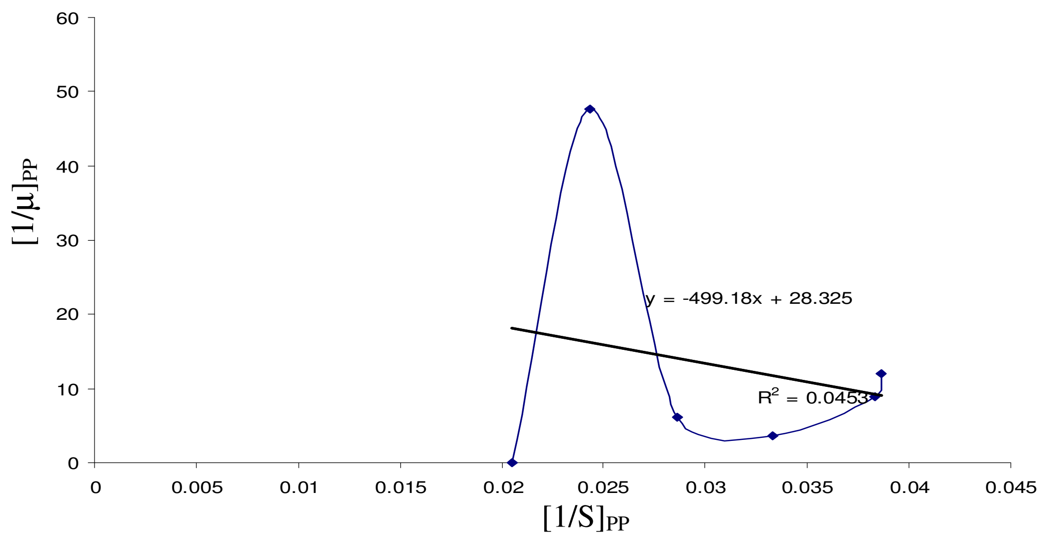

Figure 28. Graph of Line Weaver Burk plot of 1/µ versus 1/S for AIP gravity dependent

$\left[\frac{1}{\mu}\right]_{PV}$ and $\left[\frac{1}{S}\right]_{PV}$ for API gravity dependent. The behaviour of the result is similar to the result in Figure 23 with the optimum value of $\left[\frac{1}{\mu}\right]_{PV}$ at 20, obtained at 0.029, y = 276.36x – 2.1618 and R^2 = 0.0778 are the equation of best fit and square root of the curve.

Result presented in Figure 25, illustrate the relationship between $\left[\frac{1}{\mu}\right]_{PV}$ and $\left[\frac{1}{S}\right]_{PV}$ for surface tension dependent. An initial decrease in $\left[\frac{1}{\mu}\right]_{PV}$, was observed, there was also an increase which continue to a point and started decreasing again. However, the optimum value of $\left[\frac{1}{\mu}\right]_{PV}$ at 20 was obtained at the maximum value of $\left[\frac{1}{S}\right]_{PV}$, y = 44.315x + 1.8073 and R^2 = 0.8127 are the equation of best fit and square root of the curve.

Figure 26; illustrate the relationship between $\left[\frac{1}{\mu}\right]_{PP}$ and $\left[\frac{1}{S}\right]_{PP}$ for viscosity dependent. An initial

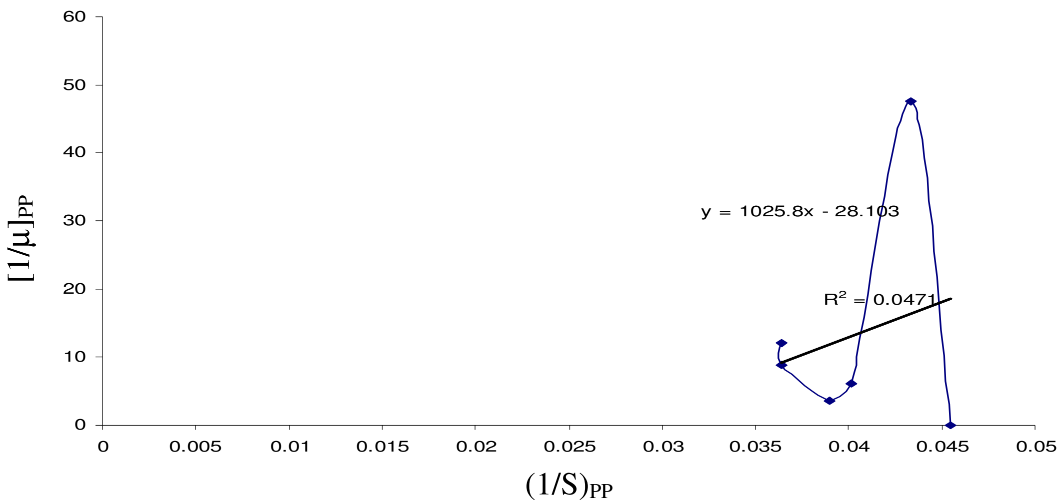

Figure 29: Graph of Line Weaver Burk plot of 1/μ versus 1/S for surface tension dependent

decrease in $\left[\frac{1}{\mu}\right]_{PP}$ was observed within 1.12 to 1.16, with a later increase in $\left[\frac{1}{\mu}\right]_{PP}$ from 1.16 to 1.22 and a further decrease within 1.22 to 1.27.

The optimum value of $\left[\frac{1}{\mu}\right]_{PP}$ at 47.62 was obtained at 1.22, y = 44.979x – 39.848 and R^2 = 0.0273 are the equation of best fit and square root of the curve.

The result presented in Figure 27, illustrate the relationship between $\left[\frac{1}{\mu}\right]_{PP}$ and $\left[\frac{1}{S}\right]_{PP}$ for density dependent. Figure 4.27 exhibit similar trend with that observed in Figure 26 with the optimum value of $\left[\frac{1}{\mu}\right]_{PP}$ at 37.62 obtained at 0.6. The equation of best fit is given as y = 7.1359x + 7.6168 with square root R^2 = 0.0046.

Figure 28, illustrate the relationship between $\left[\frac{1}{\mu}\right]_{PP}$ and $\left[\frac{1}{S}\right]_{PP}$ for API dependent increase was observed in $\left[\frac{1}{\mu}\right]_{PP}$ within 0.02 to 0.025, decrease within 0.025 to 0.033 and a further increase within 0.033 to 0.039. The optimum value of $\left[\frac{1}{\mu}\right]_{PP}$ at 47.62 was obtained at 0.024; y = -499.18x + 28.325 and R^2 = 0.0453, are the equation of best fit and square root of the curve.

Result presented in Figure 29, illustrate the relationship between $\left[\frac{1}{\mu}\right]_{PP}$ and $\left[\frac{1}{S}\right]_{PP}$ for surface tension dependent. The result exhibit similar trend with that observed in Figure 27, with the optimum value of $\left[\frac{1}{\mu}\right]_{PP}$ at 47.62 obtained at 0.043. The equation of best fit is given as y = 1025.8x – 28.103 with square root of curve R^2 = 0.0471.

CONCLUSION

The biodegradation of crude oil (petroleum hydrocarbons), was found to be a function of the various functional parameters such as density, viscosity surface tension, API gravity and temperature. Temperature was the reference functional parameter since, density viscosity; surface tension and API gravity are all dependent on the temperature the degree of degradation was measured against the change in the various functional parameters, (density, viscosity, surface tension and API gravity). The use of the change in the function parameters as a measure of the extent of degradation was done by measuring the change in the functional parameters against the growth of dynamics of the hydrocarbon-degrading microbial population as well as the higher the population growth of the microbial specie, the higher the rate of biodegradation. Conversely, a lower population growth will result in low rate of biodegradation. Conclusively this project has shown the relationship between microbial growth and the various functional parameters as function of substrate in the measurement of the extent of biodegradation.

REFERENCES

Adebusoye SA, Ilori MO, Amund OD, Teniola OD, Olatope SO (2007). "Microbial degradation of petroleum hydrocarbons in a polluted tropical stream," World J. Microbiol. and Biotechnol. vol.23, no.8, pp. 1149-1159.

Atlas RM (1981). "Microbial degradation of petroleum hydrocarbons: an environmental perspective," *Microbiological Reviews*, vol. 45, no. 1, pp. 180-209.

Atlas RM, Bartha R (1992). "Hydrocarbon biodegradation and oil spill bioremediation," *Advances in Microbial Ecology*, vol.12, pp. 287-338.

Bae H, Yamagishi T, Suwa Y (2002). Evidence for degradation of 2-chlorophenol by enrichment cultures under denitrifyind conditions. *Microbiol*. Vol.148, pp.221-227.

Barathi S, Vasudevan N (2001). "Utilization of petroleum hydrocarbons by Pseudomonas fiuorescens isolated from a petroleum-contaminated soil," *Environment International*, vol. 26, no. 5-6, pp. 413-416.

Bartha R, Bossert L (1984), "The treatment and disposal of petroleum wastes," in Petroleum Microbiology RM. Atlas, Ed., pp. 553-578, Macmillan, New York, NY USA.

Bhat A, Tsuda M, Horiike K, Nozaki M, Vaidyanathan S, Nakazawa T (1994). Identification and characterization of a new plasmid carrying genes for degradation of 2,4-dichlorophenoxyacetate from Pseudomonas ceacia CSV90, *Environ. Microbial*. Vol.60, pp.307-312.

Brooijmans RJW, Pastink MI, Siezen RJ (2009). "Hydrocarbon-degrading bacteria: the oil-spill dean-up crew," *Microbial Biotechnology*, vol. 2, no. 6, pp. 587-594.

Chailian F, Flèche A La, Bury E (2004). "Identification and biodegradation potential of tropical aerobic hydrocarbon- degrading microorganisms," *Research in Microbiology*, vol.155, no. 7, pp. 587-595.

Das K, Mukherjee AK (2007). "Crude petroleum-oil biodegradation efficiency of Bacillus subtilis and Pseudomonas aeruginosa strains isolated from a petroleum-oil contaminated soil from North-East India," *Bioresource Technology*, vol. 98, no. 7, pp. 1339-1345.

Daugulis AJ, McCracken CM (2003). "Microbial degradation of high and low molecular weight polyaromatic hydrocarbons in a two-phase partitioning bioreactor by two strains of *Sphingomonas sp*," *Biotechnology Letters*, vol. 25, no. 17, pp. 1441-1444.

Foght JM, Westlake PWS (1987). "Biodegradation of hydrocarbons in freshwater," in Oil in Freshwater Chemistry, Biolopi, Countermeasure Technology, J. H. Vandermeulen and S. R. Hrudey, Eds., pp. 2 17-230, Pergamon Press, New York, NY, USA

Holliger C, Gaspard S, Glod G (1997). "Contaminated environments in the subsurface and bioremediation: organic contaminants," *FEMS Microbiology Reviews*, vol. 20, no. 3-4, pp. 517-523.

Leahy JG, Colwell RR (1990). "Microbial degradation of hydrocarbons in the environment," *Microbiological Reviews*, vol. 54, no. 3, pp. 305-315.

Medina-Bellver JI, Mann P, Ddgado A (2005). "Evidence for in situ crude oil biodegradation after the Prestige oil spill," *Environmental Microbiology*, vol. 7, no.6, pp. 773-779.

Prince RC (1993). "Petroleum spill bioremediation in marine environments," *Critical Reviews in Microbiology*, vol. 19, no. 4, pp. 217-242.

Ukpaka C, Peter (2005). "Investigation of Microbial Influenced Corrosion in Crude Oil Storage Tanks". J. Modeling, Simulation and Control (AMSE), vol. 66, no.4, pp.1-22.

Ukpaka C, Peter (2007). "Modeling solid - gas separation in a cyclone operating system", J. Sci. and Industrial Studies, vol.5, no.1, pp.39-45.

Ukpaka C. Peter (2010). Model for the prediction of C-groups hydrocarbon remediation in activated pond system for dry season upon the influence of momentum transfer. J. Modeling, Simulation and Control AMSE), vol.71, no.2, pp. 50-70.

Ukpaka CP (2006). "Modeling the microbial thermal Kinetics system in Biodegradation of n-paraffins", J. Modeling, Simulation and Control (AMSE), vol. 67, no.1, pp.61-84.

Ukpaka CP (2009). "Development of Mathematical Correlative Model equation for the Micorbial Growth in Biodegradation of Benzylchloride in a CSTR. Knowledge Review. *A Multi-disciplinary Journal,* vol.19, no.2, pp.86-98.

Ukpaka CP (2011). "Modelling the prediction of biokinetics of dissolved oxygen for wet season degradation of petroleum hydrocarbon in pond system. Int. J. Pharma world Research, vol.2, no.3, pp.1-27.

Ukpaka CP, Nnadi VG (2008). "Smokeless Flare Modeling of an associated gas in a production oil flied", J. Modelling, Simulation and Control (AMSE), vol. 69, no.1, pp.29-46.

NOMENCLATURE

Cfu Colony forming unit

P.A *Pseudomonas alcaligenes*

P.M. *Pseudomonas mondocina*

P.S *Pseudomonas stutzeri*

P.V *Pseudomonas veroni*

P.P *Pseudomonas putida*

$\left[\frac{1}{S}\right]_{PM}$ Reciprocal of substrate for *pseudomonas mendocina*

$\left[\frac{1}{S}\right]_{PV}$ Reciprocal of substrate for *pseudomonas veronii*

$\left[\frac{1}{S}\right]_{PA}$ Reciprocal of substrate for *pseudomonas alcaligenes*

$\left[\frac{1}{S}\right]_{PV}$ Reciprocal of substrate for *pseudomonas veronii*

$\left[\frac{1}{S}\right]_{PP}$ Reciprocal of substrate for *pseudomonas putida*

$\left[\frac{1}{\mu}\right]_{PM}$ Reciprocal of specific growth rate of *pseudomonas mendocina*

$\left[\frac{1}{\mu}\right]_{PV}$ Reciprocal of specific growth rate of *pseudomonas veronii*

$\left[\frac{1}{\mu}\right]_{PS}$ Reciprocal of specific growth rate of *pseudomonas stutzeri*

$\left[\frac{1}{\mu}\right]_{PP}$ Reciprocal of specific growth rate of *pseudomonas pudida*

$\left[\frac{1}{\mu}\right]_{PA}$ Reciprocal of specific growth rate of *pseudomonas Alcaligenes*